

# Significant contrasts in aerosol acidity between China and the United States

Bingqing Zhang<sup>1</sup>, Huizhong Shen<sup>1,2</sup>, Pengfei Liu<sup>3</sup>, Hongyu Guo<sup>4</sup>, Yongtao Hu<sup>1</sup>, Yilin Chen<sup>1,2</sup>, Shaodong Xie<sup>5</sup>, Ziyang Xi<sup>5</sup>, T. Nash Skipper<sup>1</sup>, Armistead G. Russell<sup>1</sup>

<sup>1</sup>School of Civil and Environmental Engineering, Georgia Institute of Technology, Atlanta, Georgia 30332, USA

<sup>2</sup>School of Environmental Science and Engineering, Southern University of Science and Technology, Shenzhen, Guangdong 518055, China

<sup>3</sup>School of Earth and Atmospheric Sciences, Georgia Institute of Technology, Atlanta, Georgia 30332, USA

<sup>4</sup>Cooperative Institute for Research in Environmental Sciences and Department of Chemistry, University of Colorado Boulder, Boulder, Colorado 80309, USA

<sup>5</sup>College of Environmental Sciences and Engineering, State Key Joint Laboratory of Environmental Simulation and Pollution Control, Peking University, Beijing, 100871, PR China

*Correspondence to:* Huizhong Shen (shenhz@sustech.edu.cn)

**Abstract.** Aerosol acidity governs several key processes in aerosol physics and chemistry, thus affecting aerosol mass and composition, and ultimately climate and human health. Previous studies have reported aerosol pH values separately in China and the United States (US), implying different aerosol acidity between these two countries. However, there is debate about whether mass concentration or chemical composition is the more important driver of differences in aerosol acidity. A full picture of the pH difference and the underlying mechanisms responsible is hindered by the scarcity of simultaneous measurements of particle composition and gaseous species, especially in China. Here we conduct a comprehensive assessment of aerosol acidity in China and the US using extended ground-level measurements and regional chemical transport model simulations. We show that aerosol in China is significantly less acidic than in the US, with pH values 1–2 units higher. Based on a proposed multivariable Taylor Series method and a series of sensitivity tests, we identify major factors leading to the pH difference. Compared to the US, China has much higher aerosol mass concentrations (gas + particle, by a factor of 8.4 on average) and a higher fraction of total ammonia (gas + particle) in the aerosol composition. Our assessment shows that the differences in mass concentrations and chemical composition play equally important roles in driving the aerosol pH difference between China and the US — increasing the aerosol mass concentrations, but keeping the relative component contributions the same, in the US to the level in China (by a factor of 8.4) increases the aerosol pH by ~1.0 unit, and further shifting the chemical composition from US conditions to China’s that is richer in ammonia increases the aerosol pH by ~0.9 units. Therefore, both China being more polluted than the US and richer in ammonia together explain the aerosol pH difference. The difference in aerosol acidity highlighted in the present study implies potential differences in formation mechanisms, physicochemical properties, and toxicity of aerosol particles in these two countries.

## 1 Introduction

As an intrinsic aerosol property, aerosol acidity (usually characterized by aerosol pH) plays an important role in a variety of aerosol physical and chemical processes (Pye et al., 2020). Aerosol acidity can modulate aerosol mass by controlling the gas-particle partitioning of volatile and semi-volatile acids (such as HCl-Cl<sup>-</sup> and HNO<sub>3</sub>-NO<sub>3</sub><sup>-</sup>) (Guo et al., 2016) and can influence production rates of secondary aerosol through heterogeneous pathways (Jang et al., 2002; Surratt et al., 2010; Pathak et al., 2011). Acidity also affects aerosol optical properties via proton dissociation of organic functional groups (Mo et al., 2017) and the morphology or phase state of organic aerosols (Losey et al., 2016; Losey et al., 2018). Recent evidence links aerosol acidity to aerosol toxicity and health outcomes. For example, highly acidic aerosols cause greater dissolution of metals which can generate reactive oxygen

species in vivo (Fang et al., 2017). High aerosol acidity is associated with increased risks of respiratory disease and cancer (Kleinman et al., 1989; Gwynn et al., 2000; Behera et al., 2015).

Due to the difficulties in directly measuring aerosol pH (Jang et al., 2002; Li and Jang, 2012), thermodynamic models, including ISORROPIA-II (Fountoukis and Nenes, 2007), E-AIM (Clegg et al., 1998), and SCAPE2 (Kim and Seinfeld, 1995), have been widely used to calculate aerosol pH based on measured gaseous and particle composition and meteorological data such as relative humidity (RH) and temperature. Multiple studies suggest that these models can reproduce the partitioning of semi-volatile species including  $\text{HNO}_3\text{-NO}_3^-$  and  $\text{NH}_4^+\text{-NH}_3$ , which are sensitive to aerosol pH (Guo et al., 2015; Hennigan et al., 2015; Guo et al., 2016). Analyses of field observations in different regions of the United States (US) have indicated that aerosol acidity is typically high. For example, Weber et al. (2016) (Weber et al., 2016) showed that aerosol pH in the southeastern US was buffered to be consistently in the range of 0-2 despite a substantial sulfate reduction over the past 15 years, and the same trend may be applicable to other regions. Studies in the northeastern US and California also found highly acidic aerosols with mean pH values of 0.8 and 1.9, respectively (Guo et al., 2017a). Aerosol pH in the midwestern US was typically higher than other areas, with an average of 3.8 (Lawal et al., 2018). Studies in China, on the other hand, have found generally higher aerosol pH. Several studies in the heavily polluted North China Plain (NCP) region reported average pH of 3.5–5.2 (Shi et al., 2017; Ding et al., 2019; Shi et al., 2019; Song et al., 2019; Wang et al., 2020). Xi'an, a city in northwest China, had aerosol pH values up to 5 (Wang et al., 2016; Guo et al., 2017b). Some sites in southeast China had lower aerosol pH, such as the site in Guangzhou which had an average of 2.3 (Jia et al., 2020). A comprehensive, nationwide comparison of aerosol pH between China and the US can provide a better understanding of the factors driving aerosol pH and its effect on aerosol formation mechanisms and properties (Pathak et al., 2009; Guo et al., 2017a; Wang et al., 2020). However, such comparisons are still scarce (Guo et al., 2017b; Nenes et al., 2020; Zheng et al., 2020), primarily because of a lack of extensive simultaneous measurements of aerosol composition and semi-volatile gaseous compounds in China. In this study, we compared the aerosol mass concentrations, chemical composition, and acidity between China and the US based on one-year measurements from 34 ground monitoring sites in the US and 16 sites in China (mostly clustered in the NCP). In order to extend the spatial coverage to nationwide scales, we employed the Community Multiscale Air Quality (CMAQ) model to simulate the concentrations of gaseous and particle species which were used to calculate aerosol pH across both countries. We proposed a new method to identify the factors driving the pH difference between these two countries and discussed the causes and implications of the pH difference.

## 2 Data collection and method

### 2.1 Observational data

Measurements of gaseous species (including  $\text{HNO}_3$ ,  $\text{NH}_3$  and  $\text{HCl}$ ) and particle components (including  $\text{SO}_4^{2-}$ ,  $\text{NO}_3^-$ ,  $\text{NH}_4^+$ ,  $\text{Cl}^-$ , and nonvolatile cations (NVCs)) from monitoring networks in China and the US are used for analysis and comparison in this study. NVCs considered are  $\text{Na}^+$ ,  $\text{Mg}^{2+}$ ,  $\text{K}^+$ , and  $\text{Ca}^{2+}$ . The names and locations of the monitoring sites can be found in Tables S1 and S2.

The sum of total observed aerosol ionic compounds is defined as water soluble ions (WSI), though it is recognized that not all of the ions are routinely measured (e.g., trace species and organic ions). We also study the partitioning of semi-volatile species including  $\text{NH}_3\text{-NH}_4^+$  and  $\text{HNO}_3\text{-NO}_3^-$  because they are sensitive to pH, especially when the partitioning ratios,  $\epsilon(\text{NH}_4^+)$  and  $\epsilon(\text{NO}_3^-)$ , defined as the molar ratio of  $\text{NH}_4^+$  to total ammonia ( $\text{TNH}_3=\text{NH}_3+\text{NH}_4^+$ ) and the molar ratio of  $\text{NO}_3^-$  to total nitrate ( $\text{TNO}_3=\text{HNO}_3+\text{NO}_3^-$ ), are around 50% (Guo et al., 2017a; Chen et al., 2019).

In the US, observational data are from co-located Clean Air Status and Trends Network (CASTNET) (<https://www.epa.gov/castnet>) and Ammonia Monitoring Network (AMoN) (<http://nadp.slh.wisc.edu/amon/>) sites. CASTNET and AMoN sites are assumed to

be co-located if they are within 1km of one another. Observations from co-located sites are then combined for pH calculation. Weekly ambient concentrations of gases and particulate species, including  $\text{HNO}_3$ ,  $\text{SO}_4^{2-}$ ,  $\text{NO}_3^-$ ,  $\text{NH}_4^+$ ,  $\text{Cl}^-$  and NVCs, are available from CASTNET sites, while biweekly concentrations of  $\text{NH}_3$  are available from AMoN sites. To match biweekly data of  $\text{NH}_3$  from AMoN to weekly data of other species from CASTNET, the same  $\text{NH}_3$  are used for both weeks of the CASTNET samples. This assumption is expected to have a minor effect on pH estimates, as a previous study found that a 10 times increase in  $\text{NH}_3$  is required to increase pH by one unit (Guo et al., 2017b). This assumption is also supported in later discussion (Text S1). HCl data is not available, so we use particle phase  $\text{Cl}^-$  as total Cl for pH calculations. Sensitivity tests assuming HCl concentrations of four times the  $\text{Cl}^-$  concentrations or using HCl concentrations derived from CMAQ modeled HCl/ $\text{Cl}^-$  ratios show little difference in aerosol pH compared to the pH estimated by using particle phase  $\text{Cl}^-$  as total Cl (Fig. S1). Considering the small reported change in aerosol pH in the US over a long-term period (Weber et al., 2016; Lawal et al., 2018) and the configuration of the chemical transport model which is set up for the year 2011 (see the following section), we use observational data in 2011 to investigate the aerosol pH in the US. Only sites with measurements available for all species were selected for this study. There are 34 co-located CASTNET and AMoN sites, which are scattered across the contiguous US (Fig. S2a). The accuracy of CASTNET measurements has been assessed through the analysis of reference and continuing calibration verification samples with a criterion of 95-105% (except  $\text{NH}_4^+$ , whose accuracy criterion is 90-110%). Detailed information about data quality is available in the CASTNET Quality Assurance Report-Annual 2011 (United States Environmental Protection Agency, 2012b). A previous study demonstrated that the  $\text{NH}_3$  concentrations measured by the passive AMoN samplers are comparable to annular denuder systems (as a reference system) with a mean relative percent difference of -9% (Puchalski et al., 2015).

In China, hourly observational data are extracted from the data-sharing platform operated by the Comprehensive Observation Network for Air Pollution in Beijing-Tianjin-Hebei and its Surrounding Areas (<http://123.127.175.60:8765/siteui/index>). This collaborative observation network is supported by multiple institutions and provides simultaneous observations of gaseous and particle species at individual monitoring sites (Wang et al., 2019). We derive daily average concentrations of gaseous species including  $\text{NH}_3$ ,  $\text{HNO}_3$  and HCl and of particle species including  $\text{NH}_4^+$ ,  $\text{NO}_3^-$ ,  $\text{Cl}^-$ , and NVCs from hourly observational data at 16 monitoring sites for use in pH calculation. These monitoring sites are clustered in NCP in eastern China (Fig. S2c). Due to the lack of data quality information, we first process the data by removing unreasonable data points. We define a set of valid data containing all the measured components in one day as one case. We first remove cases with one or more missing components. In this step, 2704 of 5840 cases are removed. We then identify data points that are more than three median absolute deviations from the median as outliers and remove cases with any component identified as an outlier. Eventually, 1766 cases remain for subsequent analyses. Although we remove many cases in this process, the remaining cases cover most of the days in a year and are evenly distributed by month (Table S3).

It should be noted that the weekly (or longer) duration of the CASTNET samples in the US may lead to biases in the measured concentrations especially for volatile species such as ammonium nitrate. Sickles et al. (1999) conducted a comprehensive comparison of measurements using the CASTNET weekly-duration sampling approach with those using a 24-h-duration sampling approach. Both approaches used filter packs. They found that compared to 24-h sampling, weekly sampling led to low biases of -5%, -5%, and -0.7%, on average, in measured  $\text{HNO}_3$ ,  $\text{NO}_3^-$ , and  $\text{NH}_4^+$ , respectively, and high biases of 4% and 16%, on average, in  $\text{SO}_4^{2-}$  and  $\text{SO}_2$ , respectively. To evaluate the potential biases in the calculated aerosol pH due to the weekly-duration sampling, we conduct a sensitivity test to adjust the CASTNET-measured concentrations based on the reported average differences between weekly-duration and 24-h-duration samples (Sickles et al., 1999) (Results and Discussion).

## 115 2.2 Model configuration

We use CMAQ version 5.0.2 (United States Environmental Protection Agency, 2014) to simulate gaseous and particle species concentrations and aerosol pH in China and the US. The model domains cover mainland China and the contiguous US with 124×184 and 112×148 horizontal grid cells, respectively. Both are resolved at the 36-km horizontal resolution with 13 vertical layers extending to ~16 km above the ground. In both simulations, gas-phase chemistry is modeled with the CB05 chemical mechanism (Yarwood et al., 2005), and the aerosol thermodynamic equilibrium is modeled with ISORROPIA II (Fountoukis and Nenes, 2007).

The meteorological and emission inputs used to drive the China simulation are adopted from “AiMa”, an online operational air quality forecasting system (Lyu et al., 2017; AiMa Forecast, 2017). In the AiMa modeling system, the meteorological data are generated with the Weather Research and Forecasting (WRF) model (William C. Skamarock 2008) driven by the 0.5-degree global weather forecast products produced by the National Centers for Environmental Prediction (NCEP) Global Forecast System (GFS) (Global Forecast System (GFS) Model). The AiMa emission inventory was compiled and derived by integrating a variety of inventories and utilizing various activity data and has been continuously updated since its establishment (Lyu et al., 2017). The base year of the current AiMa emission inventory is 2017. For the US simulation, we use WRF-modeled meteorological fields downscaled from the North American Regional Reanalysis (NARR) data (Mesinger et al., 2006) as the meteorological input and the 2011 National Emissions Inventory provided by the US Environmental Protection Agency as the emission input (United States Environmental Protection Agency, 2012a). The base year of the meteorology and emissions is consistent with the year of the measurements in each country (i.e., 2017 for China and 2011 for the US).

In order to evaluate the model performance against observations, we calculate normalized mean bias (NMB) and normalized root-mean-square error (NRMSE) to evaluate the spatial variation of pH, species concentrations and partitioning ratios with following equations:

$$\text{NMB} = \frac{\sum_1^N (C_m - C_o)}{\sum_1^N C_o} \quad (1)$$

$$\text{NRMSE} = \frac{\sqrt{\frac{\sum_1^N (C_m - C_o)^2}{N}}}{\bar{C}_o} \quad (2)$$

where  $C_m$  is the modeled value,  $C_o$  is the observed value,  $N$  is the number of simulation-observation pairs.

## 2.3 Aerosol pH calculation

140 In this study, we use the ISORROPIA-II thermodynamic model (Fountoukis and Nenes, 2007) to determine the composition in a  $\text{K}^+$ - $\text{Ca}^{2+}$ - $\text{Mg}^{2+}$ - $\text{NH}_4^+$ - $\text{Na}^+$ - $\text{SO}_4^{2-}$ - $\text{NO}_3^-$ - $\text{Cl}^-$ - $\text{H}_2\text{O}$  aerosol system under equilibrium conditions with gas phase precursors. Aerosol pH is calculated based on  $\text{H}^+$ <sub>air</sub> and liquid water content (LWC) from ISORROPIA-II output:

$$\text{pH} = -\log_{10}(\gamma_{\text{H}^+} \cdot H_{\text{aq}}^+) = -\log_{10}\left(\frac{1000\gamma_{\text{H}^+} \cdot H_{\text{air}}^+}{\text{LWC}}\right) \quad (3)$$

145 where  $\gamma_{\text{H}^+}$  is the activity coefficient of the hydronium ion which is assumed to be 1 in this study (the binary activity coefficients of ionic pairs, including  $\text{H}^+$ , are calculated in ISORROPIA-II),  $\text{H}^+$ <sub>aq</sub> (mol L<sup>-1</sup>) is the hydronium ion concentration in aerosol liquid water,  $\text{H}^+$ <sub>air</sub> (μg m<sup>-3</sup>) is the equilibrium particle hydronium ion concentration per volume air. LWC (μg m<sup>-3</sup>) in this study only considers the water uptake by inorganic species. The effect of water uptake by organic species on aerosol pH has been found to be minor (Guo et al., 2015).

150 There are two modes in ISORROPIA-II's calculation, the forward mode and the reverse mode. In the forward mode, the inputs include total concentrations (i.e., gas+particle) of  $\text{TNH}_3$ ,  $\text{TNO}_3$ ,  $\text{TCl}$  ( $\text{HCl}+\text{Cl}^-$ ),  $\text{SO}_4$  and NVCs and meteorological parameters

(temperature and RH); in the reverse mode, only the particle phase of compounds and meteorological parameters are needed (Fountoukis and Nenes, 2007). In this study, the ISORROPIA-II model is run in the forward mode for aerosol in metastable state because the concentrations of both gas and particle species are available and also because the reverse mode has been reported to be more sensitive to measurement errors (Hennigan et al., 2015; Song et al., 2018).

155 We find that there are measurements with unrealistically high  $\text{Ca}^{2+}$  concentrations (such that  $\text{Ca}^{2+}$  is more than  $\text{LWC} \times 0.002$ , i.e., the solubility of  $\text{Ca}^{2+}$  in aerosol liquid water). This may be due to the measurement method of  $\text{Ca}^{2+}$  which uses large amounts of water to dissolve filter-collected particles. This process will likely dissolve the water-insoluble part of  $\text{Ca}^{2+}$  in aerosols which may cause higher bias in aerosol  $\text{Ca}^{2+}$  concentrations. In the existence of aerosol  $\text{SO}_4^{2-}$ ,  $\text{Ca}^{2+}$  precipitates along with  $\text{SO}_4^{2-}$  as  $\text{CaSO}_4$  because of the low solubility (Seinfeld and Pandis, 2006). Including the high  $\text{Ca}^{2+}$  concentration leads to large differences in  
160 estimated pH because of the high acidity of  $\text{SO}_4^{2-}$  (Text S2). In order to avoid this potential bias, we use modified  $\text{Ca}^{2+}$  concentration for pH calculations while keeping  $\text{SO}_4^{2-}$  unchanged. That is, we use the original  $\text{Ca}^{2+}$  concentration to calculate aerosol LWC and then use the concentration of  $\text{Ca}^{2+}$  that can dissolve in the LWC as the modified  $\text{Ca}^{2+}$  concentration in cases where the original  $\text{Ca}^{2+}$  exceeds its solubility in the calculated LWC.

We compare the directly measured gas-particle partitioning ratios of semi-volatile compounds with the ratios re-partitioned by  
165 ISORROPIA-II using measured total (gas+particle) concentrations as inputs. The purpose of this comparison, as conducted in previous studies (Guo et al., 2016; Guo et al., 2017a), is to examine the measurement data quality. This method is effective when the species have substantial fractions in both gas and particle phases (Guo et al., 2017a). The comparison results of  $\epsilon(\text{NH}_4^+)$  and  $\epsilon(\text{NO}_3^-)$  are shown in Fig. S3. The correlation coefficients and the slopes of linear regression are all close to 1, suggesting good agreement between the measured and ISORROPIA-re-calculated partitioning ratios. In terms of these partitioning ratios, the  
170 model (ISORROPIA-II) performs better in the US than in China, which may be attributable, in part, to the more balanced partitioning of the species between gas and particle phase in the US.

## 2.4 Multivariable Taylor Series Method (MTSM)

To separate the contribution of individual components (eight species in total, including  $\text{Na}^+$ ,  $\text{SO}_4$ ,  $\text{TNO}_3$ ,  $\text{TNH}_3$ ,  $\text{TCl}$ ,  $\text{Ca}^{2+}$ ,  $\text{K}^+$ , and  $\text{Mg}^{2+}$ ) and meteorological variables (RH and temperature) to the pH difference between China and the US, we propose a  
175 multivariable Taylor Series method (MTSM). First, we derive the average conditions (i.e., species concentrations and meteorological conditions) across all the sites in the US and China. We then use the US as the starting point and China as the end point and decompose the contributions of individual compounds to the pH difference based on the following equations:

$$\Delta c_i = c_{i,China} - c_{i,US} \quad (4)$$

$$c_{i,\lambda} \cong c_{i,US} + \Delta c_i \cdot \lambda \quad (5)$$

$$180 \quad \Delta pH = pH_{China} - pH_{US} = \int_0^1 \left( \sum_{i=1}^{10} \frac{\partial pH}{\partial c_{i,\lambda}} \cdot \Delta c_i \right) \cdot d\lambda \cong \sum_{s=1}^{100} \left( \sum_{i=1}^{10} \frac{\partial pH}{\partial c_{i,\frac{s}{100}}} \cdot \Delta c_i \right) \cdot 0.01 \quad (6)$$

$$\Delta pH_i \cong \sum_{s=1}^{100} \frac{\partial pH}{\partial c_{i,\frac{s}{100}}} \cdot \Delta c_i \cdot 0.01 \quad (7)$$

where subscript  $i$  denotes a specific species or meteorological variable;  $c_{i,China}$  and  $c_{i,US}$  represent the values of  $i$  in China and the US, respectively;  $\Delta c_i$  is the difference in  $c_i$  between China and the US;  $c_{i,\lambda}$  is an intervening  $c_i$  between  $c_{i,China}$  and  $c_{i,US}$  defined by  $\lambda$ ,  $\lambda \in [0, 1]$ ; when  $\lambda$  is 0,  $c_{i,\lambda}$  is  $c_{i,US}$ ; when  $\lambda$  is 1,  $c_{i,\lambda}$  is  $c_{i,China}$ . The pH difference between China and the US (i.e.,  $\Delta pH$ ) can be  
185 expressed as the sum of the partial derivatives of pH with respect to  $c_{i,\lambda}$  which is then integrated from  $c_{i,US}$  to  $c_{i,China}$ , as described by Eq. (6). In this study, we take 100 steps with equal intervals to gradually change  $\lambda$  from 0 to 1 (Eq. (6)) and record the partial derivatives of pH with respect to individual  $c_{i,\lambda}$ , and derive the contributions of all the species and meteorological variables to the

pH change at every step. By summing up the contributions of individual variables at all steps, we characterize the contributions of individual factors to the overall pH difference (Eq. (7)). Based on the same method, we further quantify the contributions of individual factors to the differences in LWC and  $H_{\text{air}}^+$ , respectively, the two variables directly used to calculate aerosol pH (Results and Discussion).

### 3 Results and discussion

#### 3.1 The pH difference between China and the US

##### 3.1.1 The pH difference based on observations

The sensitivity test to adjust the CASTNET-measured concentrations based on the reported average differences between weekly-duration and 24-h-duration samples shows little difference between the unadjusted and adjusted pH values in the US ( $2.69 \pm 0.85$  and  $2.74 \pm 0.83$  on average for the unadjusted and adjusted pH, respectively), suggesting that the weekly duration of the CASTNET sampling has little impact on the calculated aerosol pH. Therefore, we proceed with our subsequent analyses using the unadjusted pH. The aerosol pH values calculated based on observational data show a significant difference between China (most observation sites are in NCP) and the US. In China (mainly the NCP), the 2017 annual average pH at monitoring sites is 4.3, ranging from 3.3 to 5.4 with an interquartile range of 3.9–4.6. In the contiguous US, the 2011 annual average pH is 2.6, ranging from 1.9 to 3.9 with an inter-quartile range of 2.2–3.0 (Fig. 1). The t-test shows a statistically significant difference between the two groups ( $p < 0.0001$ ), suggesting that the aerosols are on average more acidic at the monitoring sites in the contiguous US than in China (NCP).

The pH difference is also illustrated by the cumulative distribution function (CDF) curves (Fig. 2, solid lines). The shapes of the CDF curves are similar in these two countries with a slightly steeper slope in the contiguous US (Fig. 2a). The pH values, however, are 1–2 units higher in China (NCP) than in the contiguous US across varying levels of cumulative frequencies in the CDF curves. In some cases, aerosols could be completely neutral in China (NCP) (the frequency is 2% for  $\text{pH} \geq 7$ ), while in the contiguous US, the pH values in all cases are below 6.

Spatially, 14 out of the 16 sampling sites in China are in the NCP (Fig. S2c) which is one of the most populous and polluted regions in China (Hu et al., 2014; Cui et al., 2020). Our pH results in this region are consistent with other studies (ranging from 3.5 to 4.6) (Liu et al., 2017; Ding et al., 2019; Ge et al., 2019). The distribution of sampling sites in the US, on the other hand, is more evenly distributed spatially. The pH values in the Midwest and California are higher than in other regions like the Southeast, in line with previous studies (Lawal et al., 2018; Chen et al., 2019). Overall, the pH level in the US is 1.7 units lower than over the NCP of China.

##### 3.1.2 The pH difference based on model simulations

To address the issue of insufficient spatial coverage of the observational data in China, we conduct simulations using CMAQ, in conjunction with the observational data, to further study the pH difference on a nationwide scale. We evaluate the model performance by comparing the modeled and observed aerosol pH values (Fig. 3), major particle and gaseous species including  $\text{SO}_4^{2-}$ ,  $\text{NO}_3^-$ ,  $\text{NH}_4^+$  and  $\text{HNO}_3$ ,  $\text{NH}_3$ , and the partitioning ratios including  $\epsilon(\text{NH}_4^+)$  and  $\epsilon(\text{NO}_3^-)$ , at monitoring sites (Figs. S4–S6).

Spatially, the model simulations generally capture the observed variations in pH, species concentrations, and partitioning ratios, although there are some notable biases (Figs. S4 and S5). In both China (NCP) and the contiguous US, the modeled  $\text{NH}_4^+$ ,  $\text{NO}_3^-$ , and  $\text{NH}_3$  are biased low while modeled  $\text{HNO}_3$  is biased high, resulting in low biases in the predicted  $\epsilon(\text{NO}_3^-)$  and  $\epsilon(\text{NH}_4^+)$ . The modeled  $\text{SO}_4^{2-}$  in both countries is biased low. Such low biases have been seen in previous studies (Fountoukis et al., 2013;

Theobald et al., 2016) and have been attributed to the spatial mismatch between the observations and simulations due to the coarse resolutions of model grid cells (usually 20–50 km resolution) (Shen et al., 2014; Wang et al., 2014a). Smaller NMBs in the US indicate a better performance, compared to China (NCP). Larger differences between observations and simulations in China (NCP) could also be caused by larger measurement uncertainties as the data in China are collected from different monitoring stations operated by individual research institutions (Wang et al., 2019) and thus lack a unified quality control, compared with data in the US, which come from national monitoring networks (United States Environmental Protection Agency; National Atmospheric Deposition Program). The co-occurrence of low biases in  $\epsilon(\text{NO}_3^-)$ , which causes lower bias in aerosol pH, and low biases in  $\epsilon(\text{NH}_4^+)$  and  $\text{SO}_4^{2-}$ , which cause higher bias in aerosol pH, likely offset each other, resulting in small biases in aerosol pH. Indeed, the simulated average pH values at observation sites ( $3.8 \pm 0.2$  in NCP, China and  $1.8 \pm 0.5$  in the contiguous US) are generally in line with the observed averages ( $4.3 \pm 0.5$  in NCP, China and  $2.6 \pm 0.5$  in the contiguous US) (Fig. 3), although the model shows a moderate low bias in both countries. The larger pH difference in the US than in China is likely due to the low bias in  $\text{TNH}_3$  to which the sensitivity of pH is found to be more pronounced in the US than in China (discussed in detail in Text S1).

With respect to the temporal variation, the model captures the seasonal trends of pH,  $\epsilon(\text{NH}_4^+)$ , and  $\epsilon(\text{NO}_3^-)$  in both countries, with lower values in summer and higher values in winter (Fig. 4). The lower temperature in winter favors the partitioning toward particle phase for semi-volatile species. Comparison of the seasonal trends of the individual aerosol components shows a better agreement in the US than in China. For example, the simulation in the US captures the trends of almost all components, though it is biased low for  $\text{SO}_4^{2-}$  and  $\text{NH}_4^+$  in summer (Fig. S6 b and h); the simulation in China misses the peaks of  $\text{SO}_4^{2-}$  in winter and  $\text{NH}_3$  in summer and has high biases for  $\text{HNO}_3$  in summer (Fig. S6 a, i, and e). Measurement-related biases may contribute to the disparity in the temporal trends between observed and modeled concentrations. The uncertainty in monthly profiles of emission estimates may also play an important role. For example, CASTNET's long sampling period could lead to a larger measurement bias in summer than in winter (Sickles and Shadwick, 2008); the large uncertainty in the current estimates of  $\text{NH}_3$  emissions in China, especially the reported underestimation of summertime emissions as indicated by an inversion analysis (Kong et al., 2019), may cause the absence of the summertime  $\text{NH}_3$  peak in the simulated trend (Fig. S6i). Further investigation is needed to better understand the factors underpinning the disparity between observations and model simulations. In spite of the various potential uncertainties, overall, the spatial and temporal evaluation suggests generally good agreement between the model simulations and observations in both countries.

In line with observations (Sect. 3.1.1), the nationwide model simulations show significant differences in aerosol acidity between the two countries. Almost all the areas in the US have aerosol pH values lower than 3 according to the CDF (Fig. 2b). Higher pH values are found in the middle and eastern US, while in the western US except California, the pH values are lower (Fig. 3). In China, a large portion of areas (87%) have aerosol pH values above 3 according to the CDF. This is especially true in eastern China which has the largest population (Fig. 3). Aerosol pH values in western and southeastern China are generally lower than in the east. It should be noted that due to the scarcity of observational data, the pH estimates in southern and western China are not evaluated. The nationwide annual average pH values in China and the US are  $2.7 \pm 0.6$  and  $0.8 \pm 0.8$  units, respectively, lower than the observation-based values due partly to the model bias but also because most of the monitoring sites are in areas with high pH (Fig. 3).

Given the adverse health impacts of ambient aerosols (Burnett et al., 2014; Freedman et al., 2019) and the potential linkage of aerosol acidity with aerosol toxicity through the solubility of redox-active metals (Oakes et al., 2012; Fang et al., 2015; Ye et al., 2018), we further calculate and compare the population-weighted averages of aerosol pH in the two countries to highlight the pH levels in densely populated areas. The population-weighted pH values are  $3.3 \pm 0.4$  and  $2.2 \pm 0.5$  in China and the US, respectively, both of which are higher than non-weighted averages, indicating that aerosols in more populous areas tend to be less acidic (Fig.

265 2b). This finding is further confirmed by the statistically significant positive correlation ( $\alpha=0.01$ ), within each country, between the aerosol pH and population density (China:  $r=0.42$ ,  $p<0.0001$ ; the US:  $r=0.28$ ,  $p<0.0001$ ). Consistent with the observation-based results, the t-test for the model simulations shows a significant difference in both the population-weighted and non-weighted aerosol pH values between the two countries ( $p<0.001$ ).

### 3.2 Causes of the aerosol pH difference

#### 3.2.1 Gaseous and particle compound profiles between China (NCP) and the contiguous US

270 We further investigate the factors leading to the pH difference. Although both observations and simulations are subject to uncertainty, we expect that observations should provide more direct and reliable evidence for this investigation. It should be noted that the monitoring sites in China were clustered in NCP and, thus, may not be representative of the whole of China. Table 1 summarizes the annual average concentrations of gaseous and particle species measured in China (NCP) and the contiguous US during the study period (China: 2017; US: 2011). For all the gaseous and ionic species (except  $\text{HNO}_3$ ), the average concentrations in China (NCP) are statistically significantly higher than those in the contiguous US. The total concentrations of WSI species in China (NCP) ( $34.4 \mu\text{g m}^{-3}$ ) are on average six times the concentrations in the contiguous US ( $5.7 \mu\text{g m}^{-3}$ ) and have greater variation, ranging from  $0.2\text{--}240 \mu\text{g m}^{-3}$ , compared to a range of  $0.1\text{--}31 \mu\text{g m}^{-3}$  in the contiguous US. Similar to other studies in China (Yao et al., 2002; Pathak et al., 2009; Zhang et al., 2013; Liu et al., 2016) and the US (Guo et al., 2015; Feng et al., 2020),  $\text{NH}_4^+$ ,  $\text{NO}_3^-$  and  $\text{SO}_4^{2-}$ , contribute more than 80% of the total WSI concentrations in both countries. The mass fractions of individual WSIs, however, differ between the two countries (Fig. 5). In China (NCP), the dominant WSI was  $\text{NO}_3^-$  (34.6%), followed by  $\text{SO}_4^{2-}$  (26.3%) and  $\text{NH}_4^+$  (25.5%). In the contiguous US in 2011,  $\text{SO}_4^{2-}$  contributed nearly half of the total WSI concentration (49.4%), and the contributions of  $\text{NO}_3^-$  and  $\text{NH}_4^+$  are comparable ( $\text{NO}_3^-$  17.6%,  $\text{NH}_4^+$  18.8%). Note that  $\text{SO}_4^{2-}$  and  $\text{NO}_3^-$  levels have been decreasing dramatically over the years, leading to decreases in  $\text{NH}_4^+$  since there is less substrate to interact with  $\text{NH}_3$  and form particulate ammonium species (Butler et al., 2016).

285 Two of the most predominant anions in aerosols,  $\text{SO}_4^{2-}$  and  $\text{NO}_3^-$  at the monitoring sites in China (NCP) are present at four and 15 times the concentrations observed in the contiguous US, respectively. The relative difference in  $\text{NO}_3^-$  between the two countries is the most significant, compared with the differences in other WSI components. Hence, the difference of the nitrate to sulfate molar ratio ( $\text{NO}_3^-/\text{SO}_4^{2-}$ ) is also significant between the two countries. The observational data show that the ratios at most monitoring sites in China (NCP) are larger than 1, and that only two sites have ratios lower but close to 1 (0.81, 0.94). On the other hand, 27 out of the 34 sites in the contiguous US show a ratio lower than 1, ranging from 0.25–0.99. High  $\text{NO}_3^-/\text{SO}_4^{2-}$  in China (NCP) could be caused by more efficient oxidation of  $\text{NO}_x$  than  $\text{SO}_2$  in China leading to greater nitrate formation as well as higher aerosol pH and availability of  $\text{NH}_3$  which favor the formation of particle nitrate (Guo et al., 2018b; Vasilakos et al., 2018). The varying ratios of  $\text{NO}_3^-/\text{SO}_4^{2-}$  on aerosol could further affect aerosol liquid water uptake, which is discussed in Supplementary Information (Text S2).

295 The most abundant cation in aerosols is  $\text{NH}_4^+$ , and the concentration difference of  $\text{NH}_4^+$  between the two countries (by a factor of 11) is more significant than the difference of other cations (by factors of 2-7). In addition,  $\epsilon(\text{NH}_4^+)$  in China (NCP) (0.13–0.48) is approximately 50% lower than in the contiguous US (0.22-0.85), meaning that compared to the US,  $\text{TNH}_3$  in China tends to be present more in the gas phase. Higher  $\text{NH}_4^+$  and lower  $\epsilon(\text{NH}_4^+)$  levels in China amount to a higher level of  $\text{TNH}_3$  which has an important influence on aerosol pH, partitioning of  $\text{TNO}_3$  and even particulate mass (see Supplementary Information for more discussion).

300 NVCs such as  $\text{Na}^+$ ,  $\text{Ca}^{2+}$ ,  $\text{Mg}^{2+}$ , and  $\text{K}^+$  are often minor components of particles but are important because of their ability to neutralize acidic species in the atmosphere, such as sulfuric and nitric acids (Zhang et al., 2007). Neglecting NVCs would cause



low biases of pH, driving the  $\text{NH}_3\text{-NH}_4^+$  equilibrium to shift toward the particle phase because more ammonium would be used to neutralize the aerosol that would otherwise be neutralized by NVCs (Guo et al., 2018a). Therefore, NVCs are included in calculating aerosol pH in this study. High NVC concentrations usually occur at the sites near emission sources. For example, high concentrations of  $\text{Na}^+$ , mainly from sea salt (Zhang et al., 2011), occur at Sites 13, 27, and 30 in the US, which are all coastal sites. High concentrations of  $\text{Ca}^{2+}$ , mainly from mineral dust, are found at Sites 6, 11, and 23 in the contiguous US and at Site 5 in China (NCP), which are in prairies impacted by sand and dust. Average NVC concentrations in China (NCP) are up to an order of magnitude higher than in the contiguous US, although in both countries, most of the NVCs concentrations are small compared to  $\text{SO}_4^{2-}$ ,  $\text{NO}_3^-$ , and  $\text{NH}_4^+$ . The predominant NVCs in China (NCP) are  $\text{Ca}^{2+}$  (2.8%),  $\text{K}^+$  (2.1%), and  $\text{Na}^+$  (2.0%), and in the contiguous US, they are  $\text{Ca}^{2+}$  (5.9%) and  $\text{Na}^+$  (3.7%).

### 3.2.2 Characterization of contributions to aerosol acidity by individual factors

We use MTSM as described in Sect. 2.4 to characterize the contribution of each component to the pH difference between the US and China. Three groups (i.e., observation, simulation non-weighted, simulation population-weighted) of the annual average concentrations in the US and China listed in Table S4 are chosen as the starting (US) and ending (China) points to perform the analysis. The results are shown in Fig. 6.

The average concentrations based on the observational and simulated data are not completely consistent due to the representativeness of the monitoring sites and the discrepancy between the simulations and observations. The MTSM analyses based on the three groups, however, show similar results. For example, all three groups suggest the high  $\text{TNH}_3$  in China as an important factor leading to the difference in aerosol pH between the two countries (Fig. 6). The contribution of  $\text{TNH}_3$  is the highest in the “observation” group due to the large difference in  $\text{TNH}_3$  concentration. Other cations, mainly NVCs, have a relatively small effect (0.2, 0.2, and 0.3 in groups “observation”, “simulation”, “simulation-weighted”, respectively), which is consistent with a previous study (Zheng et al., 2020). Unlike  $\text{TNH}_3$  and NVCs which lead to higher pH values in China than in the US,  $\text{SO}_4^{2-}$  contributes in the opposite direction to the pH difference. High  $\text{SO}_4^{2-}$  concentrations decrease aerosol pH in China by 0.6–1.3 units, compared to the US, although this effect is fully offset by  $\text{TNH}_3$ .

Compared to other species, the concentrations of  $\text{TNO}_3$  are the most different between the two countries (by a factor of 15), but MTSM shows that the contribution of  $\text{TNO}_3$  to the pH difference is relatively small (0.1, 0.1, and 0.2 in the observation, non-weighted, and population-weighted groups). This result is further confirmed by a sensitivity test of  $\text{TNO}_3$  (Fig. S10) which shows that the change in pH from changing only  $\text{TNO}_3$  is small in both countries. More detailed analyses and discussions on the effects of  $\text{TNH}_3$ ,  $\text{TNO}_3$ , and  $\text{SO}_4$  on aerosol pH can be found in Supplementary Information.

Studies have identified an important role of temperature in driving aerosol pH (Battaglia et al., 2017; Tao and Murphy, 2019; Jia et al., 2020). Our MTSM analysis shows that temperature accounts for 0.07–0.39 unit of pH difference between China and the US, which varies by group (Fig. 6). Such relatively small contributions of temperature, compared to those of  $\text{TNH}_3$  and  $\text{SO}_4$ , are mainly because of the small difference in temperature between these two countries which are at similar latitudes. The difference in the annual average temperature between China and the US is 1.4 K, -5.0 K, and 2.6 K in the observation, non-weighted, and population-weighted groups, respectively (Table S4).

### 3.2.3 Two pathways leading to the aerosol acidity difference

As aerosol pH is calculated as  $[\log_{10}(\text{LWC}) - \log_{10}(\text{H}_{\text{air}}^+) - 3]$ , all mechanisms affecting aerosol pH must be through the modification of LWC,  $\text{H}_{\text{air}}^+$ , or both (LWC and  $\text{H}_{\text{air}}^+$  are expressed as mass per unit volume of air,  $\mu\text{g m}^{-3}$ ). We quantitatively separate the contributions of individual factors to the China-US pH difference into the LWC-modifying pathway and the  $\text{H}_{\text{air}}^+$ -

modifying pathway (Fig. 6). To achieve this, we use MTSM to quantify the contributions of individual factors to the differences in  $\log_{10}(\text{LWC})$  and  $[-\log_{10}(\text{H}_{\text{air}}^+) - 3]$ , respectively, between the two countries, with the same approach as we did for pH (LWC and  $\text{H}_{\text{air}}^+$  are two output variables directly predicted by ISORROPIA). The results show that both the changes in LWC and  $\text{H}_{\text{air}}^+$  lead to increases in aerosol pH when conditions change from those in the US to China.

345 Given that LWC increases with aerosol mass concentration (Song et al., 2019), higher component concentrations in China than in the US increase LWC and, thus, increase aerosol pH (Fig. 6b). Through the LWC-modifying pathway, changes in  $\text{SO}_4$ ,  $\text{TNH}_3$ , and  $\text{TNO}_3$  lead to increases in pH (0.15–0.3) (Fig. 6b), which are consistent in all three groups. Compared to other groups, the observation group represents a higher pH increase due to Cl and a higher pH decrease due to RH (Fig. 6b), mainly because of the larger differences in Cl concentrations and RH for this group than for other groups (Table S4).

350 Through the  $\text{H}_{\text{air}}^+$ -modifying pathway, the effects of individual factors on pH changes vary (Fig. 6c). Increases in acidic components ( $\text{SO}_4$  and  $\text{TNO}_3$ ) increase  $\text{H}_{\text{air}}^+$  and thus decrease aerosol pH (Fig. 6c). Increases in  $\text{TNH}_3$ , TCl, and NVCs, on the other hand, decrease  $\text{H}_{\text{air}}^+$  and increase aerosol pH (Fig. 6c). By increasing  $\text{H}_{\text{air}}^+$ , increased  $\text{SO}_4$  decreases pH by 0.7–1.2 units, showing a much stronger acidic capacity than another acidic component,  $\text{TNO}_3$ , which only decreases pH by 0.17–0.27 units (Fig. 6c). Compared to the US, China is in a  $\text{TNH}_3$ -rich condition. The molar ratios of  $[\text{TNH}_3] / (2 \times [\text{SO}_4] + [\text{TNO}_3] + [\text{TCl}])$  in China vs. in the US  
355 are 3 vs. 1.4, 2.0 vs. 1.0, and 2.4 vs. 1.5 in the observation, non-weighted, and population-weighted groups, respectively. Changing the conditions from the US to China,  $\text{TNH}_3$  plays the most important role in neutralizing the acidic components and driving the pH increase in the  $\text{H}_{\text{air}}^+$ -modifying pathway (Fig. 6c).

For individual factors, the net changes in pH are a result of the combination of the two pathways. For example, increased  $\text{SO}_4$  increases LWC and  $\text{H}_{\text{air}}^+$  simultaneously. The increase in LWC increases aerosol pH, while the increase in  $\text{H}_{\text{air}}^+$  decreases aerosol  
360 pH. All three groups suggest that the effect of  $\text{H}_{\text{air}}^+$  on pH overwhelms that of LWC on pH, leading to a net decrease in pH from an  $\text{SO}_4$  increase (Fig. 6). Increased  $\text{TNH}_3$  increases pH in both pathways, adding up to a larger increase in pH (Fig. 6). Increased  $\text{TNO}_3$  through these two pathways, however, is associated with opposite effects on pH which are comparable in magnitude and thus tends to offset each other (especially in the observation group) (Fig. 6). This explains the aforementioned small change in pH from the  $\text{TNO}_3$  increases. Combining all the factors, both pathways increase aerosol pH (Fig. 6b and c), resulting in the large  
365 difference in aerosol acidity between these two countries (Fig. 6a).

To facilitate a follow-up sensitivity test to link the two pathways with mass concentration and chemical composition, we define the total mass concentration as the sum of the mass concentrations of all the eight input components (i.e.,  $\text{Na}^+$ ,  $\text{SO}_4$ ,  $\text{TNH}_3$ ,  $\text{TNO}_3$ , TCl,  $\text{Ca}^{2+}$ ,  $\text{K}^+$ , and  $\text{Mg}^{2+}$ ), including both gas and particle phases, and the chemical composition as the composition of the eight components in the aerosol (gas + particle) system. The observation group shows that the total mass concentration in China is 8.4  
370 times that in the US, and the chemical composition in China is richer in  $\text{TNH}_3$  than that in the US (as illustrated by the ratios of  $[\text{TNH}_3] / (2 \times [\text{SO}_4] + [\text{TNO}_3] + [\text{TCl}])$  mentioned above). It has been found that both LWC and  $\text{H}_{\text{air}}^+$  are affected by mass concentration and aerosol composition (Guo et al., 2015; Zheng et al., 2020; Xie et al., 2020). To investigate how the differences in mass concentration and composition between China and the US is associated with the LWC- and  $\text{H}_{\text{air}}^+$ -modifying pathways and consequently the pH difference, we first increase the mass concentrations of individual input components in the US case by a  
375 constant factor of 8.4, whereby we get an intervening case representing the overall pollution level as in China but with the chemical composition feature as in the US (Table S4, sensitivity test). From the intervening case, we then shift the composition of the US case to that of China (Table S4, sensitivity test). Note that throughout this sensitivity test, meteorological conditions are held constant. The first step by increasing the mass concentration yields an increase of 1.02 units in the aerosol pH, which is mainly achieved through the LWC-modifying pathway (1.06 units) instead of the  $\text{H}_{\text{air}}^+$ -modifying pathway (-0.04 unit) (Fig. S7 (a), (b),  
380 (c)). The second step that changes the chemical composition shows a further increase of 0.76 units in the aerosol pH, which is

mainly achieved through the  $H_{\text{air}^+}$ -modifying pathway (0.88 units). The LWC-modifying pathway plays a minor role (-0.11 unit) in this step (Fig. S7 (d), (e), (f)). This sensitivity test reveals that the LWC-modifying pathway is mainly associated with the change in mass concentration, and the  $H_{\text{air}^+}$ -modifying pathway is mainly associated with the change in chemical composition.

It is surprising that in the first step, pH changed when the concentrations of all chemical components were scaled by a common factor. This means that pH changes with mass concentration of the aerosol (gas+particle) even though all chemical component mole fractions hold. Further investigation shows that, increasing the aerosol concentration drives TNO<sub>3</sub> and TNH<sub>3</sub> partitioning toward particle phases— $\epsilon(\text{NH}_4^+)$  and  $\epsilon(\text{NO}_3^-)$  increase from 0.4 and 0.6 to 0.6 and 0.98, respectively. Given the weak acidity of NO<sub>3</sub><sup>-</sup>, the particle is ultimately neutralized by the increased NH<sub>4</sub><sup>+</sup>. The repartitioning in response to the increase in mass concentration is thus key to the pH shift and can be explained by the Henry's Law, i.e.,  $[\text{A}_{\text{aq}}]=H_{\text{A}}p_{\text{A}}$ , where  $[\text{A}_{\text{aq}}]$  is the aqueous-phase concentration of component A in the unit of moles per liter water,  $p_{\text{A}}$  is the partial pressure of A in the gas phase, and  $H_{\text{A}}$  is the Henry's law coefficient (Seinfeld and Pandis, 2006).  $[\text{A}_{\text{aq}}]$  is proportional to  $c_{\text{A}} / \text{LWC}$  ( $c_{\text{A}}$  denotes the particle-phase concentration of A, note that LWC and  $c_{\text{A}}$  are expressed as mass per unit volume of air, and  $[\text{A}_{\text{aq}}]$  is expressed as moles per unit volume of water). Increasing the concentrations of all chemical components by a common factor increases  $p_{\text{A}}$  (due to the increase in the gas-phase concentration of A) but does not change  $[\text{A}_{\text{aq}}]$  (because both  $c_{\text{A}}$  and LWC increases in the same direction by the same magnitude). According to the Henry's Law, more gas-phase A will thus shift toward the particle phase to achieve a thermodynamic equilibrium of the new system.

We find that by increasing the concentration of every component by a constant factor, the magnitude and direction of the resulting change in pH are sensitive to the fraction of TNH<sub>3</sub> in the aerosol system while insensitive to the ratio of SO<sub>4</sub> to TNO<sub>3</sub>. Based on an NH<sub>4</sub><sup>+</sup>-SO<sub>4</sub><sup>2-</sup>-NO<sub>3</sub><sup>-</sup>-H<sub>2</sub>O system, we conduct a series of sensitivity tests to investigate the change in aerosol pH in response to the multiplication of a constant factor of 8.4 (Fig. S8). The change in pH reduces gradually from 1.2 units to 0.8 units when the TNH<sub>3</sub> mass fraction of the system decreases from 67% to 27% (Fig. S8). With further decreases in the TNH<sub>3</sub> fraction, the increase in pH diminishes rapidly, becomes negative when the TNH<sub>3</sub> mass fraction is lower than 25%, and is -0.6 when the TNH<sub>3</sub> mass fraction is 17% (Fig. S8). Under a constant TNH<sub>3</sub> mass fraction, the change in pH remain generally constant across a wide range of the mass ratios of SO<sub>4</sub> to TNO<sub>3</sub> (from 5:1 to 1:5) (Fig. S8). In populated continental regions, mass fractions of TNH<sub>3</sub> are often high (Bencs et al., 2008; Behera and Sharma, 2010; Zheng et al., 2015; Cheng et al., 2016; Guo et al., 2017b), and an increase in mass concentration thus typically increases the aerosol pH.

Such an assessment by tracking pathway- and step-specific contributions provides a better understanding of the pH difference between China and the US. We show that through the LWC-modifying pathway, the increases in aerosol components consistently lead to increases in pH, and that through the  $H_{\text{air}^+}$ -modifying pathway, the effects of different components on pH vary in direction. If the LWC-modifying pathway dominated the pH changes over the  $H_{\text{air}^+}$ -modifying pathway, aerosol mass concentrations would be the main factor driving the aerosol acidity difference between China and the US, and one could simply attribute the difference in aerosol acidity to the fact that China is more polluted than the US. In contrast, if the  $H_{\text{air}^+}$ -modifying pathway dominated, chemical composition would be the dominant factor, and the compound profiles of precursors emissions, which affect the fractions of the corresponding aerosol components in the air, would play an important role. While there has been debate about whether mass concentration or chemical composition plays a more important role in determining aerosol pH (Cheng et al., 2016; Guo et al., 2017a; Pye et al., 2020; Zheng et al., 2020), our results suggest that both are important in explaining the China-US pH difference (Fig. 6b and c). The three groups are not consistent with each other in which pathway contributes more than the other to the pH difference, but they all suggest that the two pathways are comparable in terms of their effects on aerosol pH (Fig. 6b and c).

Our results, showing the importance of both mass concentrations associated with LWC and chemical composition associated with  $H_{\text{air}^+}$  and a minor role of temperature, seem in some aspects to contradict a previous study (Zheng et al., 2020) which highlighted

LWC and temperature instead of chemical composition as the most important factors explaining the pH difference between China (NCP) and the US. We note that the difference in the conclusions is reasonable when considering the differences in the specific cases examined in these two studies. The previous study compared the conditions in NCP in winter with those in the southeastern US in summer (SE-US). Because of the differences in latitude (north for China vs south for the US) and season (winter for China vs summer for the US), the difference in temperature between their scenarios (29 K) was an order of magnitude greater than those in our study, which has greater spatial and temporal coverage (2.6 K in the observation group, 5 K in the non-weighted group, and -1.4 K in the population-weighted group). Using MTSM, we evaluate the pH difference between NCP and SE-US scenarios considered in the previous study. The results show that temperature accounts for 1.3 units of difference in aerosol pH between their two scenarios (Fig. S9), in line with what was previously reported (1.6 units).

In addition, ISORROPIA simulations show a LWC difference of  $8.2 \mu\text{g m}^{-3}$  between China (NCP) and the contiguous US in the “observation” group in our study and  $340 \mu\text{g m}^{-3}$  between the scenarios considered in the previous study. The much larger LWC difference in the previous study compared to ours is mainly driven by the differences in pollutant concentrations. For example, the  $\text{SO}_4$  concentration is as high as  $156 \mu\text{g m}^{-3}$  in the NCP scenario in the previous study but only  $9.2 \mu\text{g m}^{-3}$  in our study. Such differences in concentrations are reasonable, given that the previous study selected a severe haze event occurring in Beijing in winter 2013 as the scenario for China (NCP), while we use annual average levels over NCP in 2017 as our case for China (NCP). Note that winter 2013 was a period when air pollution reportedly reached record high levels across northern China (Wang et al., 2014b; Li et al., 2016). Since 2013, China has launched strict controls on air pollutant emissions, and  $\text{PM}_{2.5}$  levels have decreased significantly between 2013 and 2017 (Zhang et al., 2019). Therefore, the NCP scenario in the previous study should be more representative of short-term haze events in the pre-2013 period, while our China (NCP) case should be more representative of annual average levels in recent years.

#### 4 Conclusion and implications

Based on extended ground-level measurements and regional air quality model simulations, we find significant differences in aerosol pH between China and the US. Aerosols in the US are on average more acidic with pH generally 1–2 units lower than in China. We propose an MTSM method to identify the key factors leading to the pH difference. The MTSM analysis reveals the important role of  $\text{TNH}_3$  in causing the pH difference and an opposing effect from  $\text{SO}_4$ , which partially offsets the positive effect of  $\text{TNH}_3$  on the pH change. Other factors play relatively minor roles. Further investigation highlights two pathways related to the pH difference, one associated with changes in LWC and the other with changes in  $\text{H}_{\text{air}}^+$ . The increased mass concentration in China, compared to the US, enhances LWC, and the change in chemical composition toward a  $\text{TNH}_3$ -rich condition reduces  $\text{H}_{\text{air}}^+$ . Both pathways facilitate the increases in aerosol pH in China and are comparable in terms of driving the pH increase.

Previous studies have suggested that low aerosol pH is associated with increased toxicity because of the increased solubility of transition metals in aerosol LWC, which induce airway injury and inflammation through the production of reactive oxygen species in vivo (Kim et al., 2015). The lower aerosol pH in the US than in China implies that aerosols in the US may be more toxic than in China. However, this implication should be interpreted with caution because there are other known pathways through which particulate matter can harm humans, and the mechanisms of how particulate matter affects health are not completely understood (Armstrong et al., 2004). More studies are needed to assess the health outcomes associated with the disparity in aerosol pH between the two countries.

## Author contribution

460 HS initiated the research project. HS ran the model. HS and BZ designed the experiments, analysed results, and wrote the initial draft of the manuscript. YH, SX, and ZX helped with data preparation. All co-authors commented on and contributed to the writing of the paper.

## Competing interests

The authors declare that they have no conflict of interest.

## Data availability

465 The data presented in this manuscript and the observational data in China can be obtained from the corresponding author upon request. The observational data in China can also be obtained from the Data-sharing platform by Comprehensive Observation Network for Air Pollution in Beijing-Tianjin-Hebei and its Surrounding Areas (<http://123.127.175.60:8765/siteui/index>). The observational data in the US can be obtained from Clean Air Status and Trends Network (CASTNET) (<https://www.epa.gov/castnet>) and Ammonia Monitoring Network (AMoN) (<http://nadp.slh.wisc.edu/amon/>)

## Acknowledgements

470 This research is supported by the U.S. Environmental Protection Agency (EPA grant number R835880), the National Science Foundation (NSF SRN grant number 1444745), and partially funded by the National Air Pollution Prevention Joint Research Center of China (grant number DQGG0204). Its contents are solely the responsibility of the grantee and do not necessarily represent the official views of the supporting agencies. Further, the US government does not endorse the purchase of any commercial products or services mentioned in the publication.

475

## References

- 480 AiMa Air Quality Forecasting System: [http://www.aimayubao.com/wryb\\_eval.php?movie=no](http://www.aimayubao.com/wryb_eval.php?movie=no), 2017.
- Armstrong, B., Hutchinson, E., Unwin, J., and Fletcher, T.: Lung cancer risk after exposure to polycyclic aromatic hydrocarbons: a review and meta-analysis, *Environ Health Perspect*, 112, 970-978, 10.1289/ehp.6895, 2004.
- Battaglia, M. A., Douglas, S., and Hennigan, C. J.: Effect of the Urban Heat Island on Aerosol pH, *Environ Sci Technol*, 51, 13095-13103, 10.1021/acs.est.7b02786, 2017.
- 485 Behera, S. N., and Sharma, M.: Investigating the potential role of ammonia in ion chemistry of fine particulate matter formation for an urban environment, *Science of The Total Environment*, 408, 3569-3575, <https://doi.org/10.1016/j.scitotenv.2010.04.017>, 2010.

- Behera, S. N., Cheng, J., Huang, X., Zhu, Q., Liu, P., and Balasubramanian, R.: Chemical composition and acidity of size-fractionated inorganic aerosols of 2013-14 winter haze in Shanghai and associated health risk of toxic elements, *Atmospheric Environment*, 122, 259-271, <https://doi.org/10.1016/j.atmosenv.2015.09.053>, 2015.
- 490 Bencs, L., Khaiwal, R., Hoog, J., Rasoazanany, E., Deutsch, F., Bleux, N., Berghmans, P., Roekens, E., Krata, A., and Van Grieken, R.: Mass and ionic composition of atmospheric fine particles over Belgium and their relation with gaseous air pollutants, *Journal of Environmental Monitoring*, 10, 1148-1157, 10.1039/B805157G, 2008.
- 495 Burnett, R. T., Pope, C. A., 3rd, Ezzati, M., Olives, C., Lim, S. S., Mehta, S., Shin, H. H., Singh, G., Hubbell, B., Brauer, M., Anderson, H. R., Smith, K. R., Balmes, J. R., Bruce, N. G., Kan, H., Laden, F., Prüss-Ustün, A., Turner, M. C., Gapstur, S. M., Diver, W. R., and Cohen, A.: An integrated risk function for estimating the global burden of disease attributable to ambient fine particulate matter exposure, *Environ Health Perspect*, 122, 397-403, 10.1289/ehp.1307049, 2014.
- Butler, T., Vermeylen, F., Lehmann, C. M., Likens, G. E., and Puchalski, M.: Increasing ammonia concentration trends in large regions of the USA derived from the NADP/AMoN network, *Atmospheric Environment*, 146, 132-140, <https://doi.org/10.1016/j.atmosenv.2016.06.033>, 2016.
- 500 Chen, Y. L., Shen, H. Z., and Russell, A. G.: Current and Future Responses of Aerosol pH and Composition in the US to Declining SO<sub>2</sub> Emissions and Increasing NH<sub>3</sub> Emissions, *Environ Sci Technol*, 53, 9646-9655, 10.1021/acs.est.9b02005, 2019.
- Cheng, Y., Zheng, G., Wei, C., Mu, Q., Zheng, B., Wang, Z., Gao, M., Zhang, Q., He, K., Carmichael, G., Pöschl, U., and Su, H.: Reactive nitrogen chemistry in aerosol water as a source of sulfate during haze events in China, *Science Advances*, 2, e1601530, [10.1126/sciadv.1601530](https://doi.org/10.1126/sciadv.1601530), 2016.
- 505 Clegg, S. L., Brimblecombe, P., and Wexler, A. S.: Thermodynamic Model of the System H<sup>+</sup>-NH<sub>4</sub><sup>+</sup>-SO<sub>4</sub><sup>2-</sup>-NO<sub>3</sub><sup>-</sup>-H<sub>2</sub>O at Tropospheric Temperatures, *The Journal of Physical Chemistry A*, 102, 2137-2154, 10.1021/jp973042r, 1998.
- Cui, Y., Yin, Y., Chen, K., Zhang, X., Kuang, X., Jiang, H., Wang, H., Zhen, Z., and He, C.: Characteristics and sources of WSI in North China Plain: A simultaneous measurement at the summit and foot of Mount Tai, *Journal of Environmental Sciences*, 92, 264-277, <https://doi.org/10.1016/j.jes.2020.02.017>, 2020.
- 510 Ding, J., Zhao, P., Su, J., Dong, Q., Du, X., and Zhang, Y.: Aerosol pH and its driving factors in Beijing, *Atmos. Chem. Phys.*, 19, 7939-7954, 10.5194/acp-19-7939-2019, 2019.
- Fang, T., Guo, H., Verma, V., Peltier, R. E., and Weber, R. J.: PM<sub>2.5</sub> water-soluble elements in the southeastern United States: automated analytical method development, spatiotemporal distributions, source apportionment, and implications for health studies, *Atmos. Chem. Phys.*, 15, 11667-11682, 10.5194/acp-15-11667-2015, 2015.
- 515 Fang, T., Guo, H., Zeng, L., Verma, V., Nenes, A., and Weber, R. J.: Highly Acidic Ambient Particles, Soluble Metals, and Oxidative Potential: A Link between Sulfate and Aerosol Toxicity, *Environ Sci Technol*, 51, 2611-2620, 10.1021/acs.est.6b06151, 2017.
- Feng, J., Chan, E., and Vet, R.: Air quality in the eastern United States and Eastern Canada for 1990–2015: 25 years of change in response to emission reductions of SO<sub>2</sub> and NO<sub>x</sub> in the region, *Atmos. Chem. Phys.*, 20, 3107-3134, 10.5194/acp-20-3107-2020, 2020.
- 520 Fountoukis, C., and Nenes, A.: ISORROPIA II: a computationally efficient thermodynamic equilibrium model for K<sup>+</sup>-Ca<sup>2+</sup>-Mg<sup>2+</sup>-NH<sub>4</sub><sup>+</sup>-Na<sup>+</sup>-SO<sub>4</sub><sup>2-</sup>-NO<sub>3</sub><sup>-</sup>-Cl<sup>-</sup>-H<sub>2</sub>O aerosols, *Atmos. Chem. Phys.*, 7, 4639-4659, 10.5194/acp-7-4639-2007, 2007.
- Fountoukis, C., Koraj, D., Van Der Gon, H. D., Charalampidis, P., Pilinis, C., and Pandis, S.: Impact of grid resolution on the predicted fine PM by a regional 3-D chemical transport model, *Atmos. Environ.*, 68, 24-32, 2013.
- 525 Freedman, M. A., Ott, E.-J. E., and Marak, K. E.: Role of pH in Aerosol Processes and Measurement Challenges, *The Journal of Physical Chemistry A*, 123, 1275-1284, 10.1021/acs.jpca.8b10676, 2019.

- Ge, B., Xu, X., Ma, Z., Pan, X., Wang, Z., Lin, W., Ouyang, B., Xu, D., Lee, J., Zheng, M., Ji, D., Sun, Y., Dong, H., Squires, F. A., Fu, P., and Wang, Z.: Role of Ammonia on the Feedback Between AWC and Inorganic Aerosol Formation During Heavy Pollution in the North China Plain, *Earth and Space Science*, 6, 1675-1693, 10.1029/2019EA000799, 2019.
- 530 NCEP Product Inventory - Global Products: <https://www.nco.ncep.noaa.gov/pmb/products/gfs/#GFS>.
- Guo, H., Xu, L., Bougiatioti, A., Cerully, K. M., Capps, S. L., Hite Jr, J. R., Carlton, A. G., Lee, S. H., Bergin, M. H., Ng, N. L., Nenes, A., and Weber, R. J.: Fine-particle water and pH in the southeastern United States, *Atmos. Chem. Phys.*, 15, 5211-5228, 10.5194/acp-15-5211-2015, 2015.
- 535 Guo, H., Sullivan, A. P., Campuzano-Jost, P., Schroder, J. C., Lopez-Hilfiker, F. D., Dibb, J. E., Jimenez, J. L., Thornton, J. A., Brown, S. S., Nenes, A., and Weber, R. J.: Fine particle pH and the partitioning of nitric acid during winter in the northeastern United States, *Journal of Geophysical Research: Atmospheres*, 121, 3355-3376, 10.1002/2016jd025311, 2016.
- Guo, H., Liu, J., Froyd, K., Robert, J., Veres, P., Hayes, P., Jimenez, J., Nenes, A., and Weber, R.: Fine particle pH and gas-particle phase partitioning of inorganic species in Pasadena, California, during the 2010 CalNex campaign, *Atmospheric Chemistry and Physics Discussions*, 1-33, 10.5194/acp-2016-1158, 2017a.
- 540 Guo, H., Weber, R. J., and Nenes, A.: High levels of ammonia do not raise fine particle pH sufficiently to yield nitrogen oxide-dominated sulfate production, *Scientific Reports*, 7, 12109, 10.1038/s41598-017-11704-0, 2017b.
- Guo, H., Nenes, A., and Weber, R. J.: The underappreciated role of nonvolatile cations in aerosol ammonium-sulfate molar ratios, *Atmos. Chem. Phys.*, 18, 17307-17323, 10.5194/acp-18-17307-2018, 2018a.
- 545 Guo, H., Otjes, R., Schlag, P., Kiendler-Scharr, A., Nenes, A., and Weber, R. J.: Effectiveness of ammonia reduction on control of fine particle nitrate, *Atmos. Chem. Phys.*, 18, 12241-12256, 10.5194/acp-18-12241-2018, 2018b.
- Gwynn, R. C., Burnett, R. T., and Thurston, G. D.: A time-series analysis of acidic particulate matter and daily mortality and morbidity in the Buffalo, New York, region, *Environ Health Perspect*, 108, 125-133, 10.1289/ehp.00108125, 2000.
- Hennigan, C. J., Izumi, J., Sullivan, A. P., Weber, R. J., and Nenes, A.: A critical evaluation of proxy methods used to estimate the acidity of atmospheric particles, *Atmos. Chem. Phys.*, 15, 2775-2790, 10.5194/acp-15-2775-2015, 2015.
- 550 Hu, J., Wang, Y., Ying, Q., and Zhang, H.: Spatial and temporal variability of PM<sub>2.5</sub> and PM<sub>10</sub> over the North China Plain and the Yangtze River Delta, China, *Atmospheric Environment*, 95, 598-609, <https://doi.org/10.1016/j.atmosenv.2014.07.019>, 2014.
- Jang, M., Czoschke, N. M., Lee, S., and Kamens, R. M.: Heterogeneous Atmospheric Aerosol Production by Acid-Catalyzed Particle-Phase Reactions, *Science*, 298, 814, 10.1126/science.1075798, 2002.
- 555 Jia, S., Chen, W., Zhang, Q., Krishnan, P., Mao, J., Zhong, B., Huang, M., Fan, Q., Zhang, J., Chang, M., Yang, L., and Wang, X.: A quantitative analysis of the driving factors affecting seasonal variation of aerosol pH in Guangzhou, China, *Science of The Total Environment*, 725, 138228, <https://doi.org/10.1016/j.scitotenv.2020.138228>, 2020.
- Kim, K.-H., Kabir, E., and Kabir, S.: A review on the human health impact of airborne particulate matter, *Environment International*, 74, 136-143, <https://doi.org/10.1016/j.envint.2014.10.005>, 2015.
- 560 Kim, Y. P., and Seinfeld, J. H.: Atmospheric Gas-Aerosol Equilibrium: III. Thermodynamics of Crustal Elements Ca<sup>2+</sup>, K<sup>+</sup>, and Mg<sup>2+</sup>, *Aerosol Science and Technology*, 22, 93-110, 10.1080/02786829408959730, 1995.
- Kleinman, M. T., Phalen, R. F., Mautz, W. J., Mannix, R. C., McClure, T. R., and Crocker, T. T.: Health effects of acid aerosols formed by atmospheric mixtures, *Environ Health Perspect*, 79, 137-145, 10.1289/ehp.8979137, 1989.
- Kong, L., Tang, X., Zhu, J., Wang, Z., Pan, Y., Wu, H., Wu, L., Wu, Q., He, Y., Tian, S., Xie, Y., Liu, Z., Sui, W., Han, L., and Carmichael, G.: Improved Inversion of Monthly Ammonia Emissions in China Based on the Chinese Ammonia Monitoring Network and Ensemble Kalman Filter, *Environ Sci Technol*, 53, 12529-12538, 10.1021/acs.est.9b02701, 2019.
- 565

- Lawal, A. S., Guan, X., Liu, C., Henneman, L. R. F., Vasilakos, P., Bhogineni, V., Weber, R. J., Nenes, A., and Russell, A. G.: Linked Response of Aerosol Acidity and Ammonia to SO<sub>2</sub> and NO<sub>x</sub> Emissions Reductions in the United States, *Environ Sci Technol*, 52, 9861-9873, 10.1021/acs.est.8b00711, 2018.
- 570 Li, J., and Jang, M.: Aerosol Acidity Measurement Using Colorimetry Coupled With a Reflectance UV-Visible Spectrometer, *Aerosol Science and Technology*, 46, 833-842, 10.1080/02786826.2012.669873, 2012.
- Li, S., Ma, Z., Xiong, X., Christiani, D. C., Wang, Z., and Liu, Y.: Satellite and Ground Observations of Severe Air Pollution Episodes in the Winter of 2013 in Beijing, China, *Aerosol and Air Quality Research*, 16, 977-989, 10.4209/aaqr.2015.01.0057, 2016.
- 575 Liu, M., Song, Y., Zhou, T., Xu, Z., Yan, C., Zheng, M., Wu, Z., Hu, M., Wu, Y., and Zhu, T.: Fine particle pH during severe haze episodes in northern China, *Geophysical Research Letters*, 44, 5213-5221, 10.1002/2017GL073210, 2017.
- Liu, P., Zhang, C., Mu, Y., Liu, C., Xue, C., Ye, C., Liu, J., Zhang, Y., and Zhang, H.: The possible contribution of the periodic emissions from farmers' activities in the North China Plain to atmospheric water-soluble ions in Beijing, *Atmos. Chem. Phys.*, 16, 10097-10109, 10.5194/acp-16-10097-2016, 2016.
- 580 Losey, D. J., Parker, R. G., and Freedman, M. A.: pH Dependence of Liquid-Liquid Phase Separation in Organic Aerosol, *The Journal of Physical Chemistry Letters*, 7, 3861-3865, 10.1021/acs.jpcclett.6b01621, 2016.
- Losey, D. J., Ott, E.-J. E., and Freedman, M. A.: Effects of High Acidity on Phase Transitions of an Organic Aerosol, *The Journal of Physical Chemistry A*, 122, 3819-3828, 10.1021/acs.jpca.8b00399, 2018.
- Lyu, B., Zhang, Y., and Hu, Y.: Improving PM<sub>2.5</sub> Air Quality Model Forecasts in China Using a Bias-Correction Framework, *Atmosphere*, 8, 10.3390/atmos8080147, 2017.
- 585 Mesinger, F., DiMego, G., Kalnay, E., Mitchell, K., Shafran, P. C., Ebisuzaki, W., Jović, D., Woollen, J., Rogers, E., Berbery, E. H., Ek, M. B., Fan, Y., Grumbine, R., Higgins, W., Li, H., Lin, Y., Manikin, G., Parrish, D., and Shi, W.: North American Regional Reanalysis, *Bulletin of the American Meteorological Society*, 87, 343-360, 10.1175/bams-87-3-343, 2006.
- Mo, Y., Li, J., Liu, J., Zhong, G., Cheng, Z., Tian, C., Chen, Y., and Zhang, G.: The influence of solvent and pH on determination of the light absorption properties of water-soluble brown carbon, *Atmospheric Environment*, 161, 90-98, <https://doi.org/10.1016/j.atmosenv.2017.04.037>, 2017.
- National Atmospheric Deposition Program: Ammonia Monitoring Network (AMoN), in, <http://nadp.slh.wisc.edu/AMoN/>.
- Nenes, A., Pandis, S. N., Weber, R. J., and Russell, A.: Aerosol pH and liquid water content determine when particulate matter is sensitive to ammonia and nitrate availability, *Atmos. Chem. Phys.*, 20, 3249-3258, 10.5194/acp-20-3249-2020, 2020.
- 595 Oakes, M., Ingall, E. D., Lai, B., Shafer, M. M., Hays, M. D., Liu, Z. G., Russell, A. G., and Weber, R. J.: Iron Solubility Related to Particle Sulfur Content in Source Emission and Ambient Fine Particles, *Environ Sci Technol*, 46, 6637-6644, 10.1021/es300701c, 2012.
- Pathak, R. K., Wu, W. S., and Wang, T.: Summertime PM<sub>2.5</sub> ionic species in four major cities of China: nitrate formation in an ammonia-deficient atmosphere, *Atmos. Chem. Phys.*, 9, 1711-1722, 10.5194/acp-9-1711-2009, 2009.
- 600 Pathak, R. K., Wang, T., Ho, K. F., and Lee, S. C.: Characteristics of summertime PM<sub>2.5</sub> organic and elemental carbon in four major Chinese cities: Implications of high acidity for water-soluble organic carbon (WSOC), *Atmospheric Environment*, 45, 318-325, <https://doi.org/10.1016/j.atmosenv.2010.10.021>, 2011.
- Puchalski, M. A., Rogers, C. M., Baumgardner, R., Mishoe, K. P., Price, G., Smith, M. J., Watkins, N., and Lehmann, C. M.: A statistical comparison of active and passive ammonia measurements collected at Clean Air Status and Trends Network (CASTNET) sites, *Environmental Science: Processes & Impacts*, 17, 358-369, 10.1039/C4EM00531G, 2015.
- 605



- Pye, H. O. T., Nenes, A., Alexander, B., Ault, A. P., Barth, M. C., Clegg, S. L., Collett Jr, J. L., Fahey, K. M., Hennigan, C. J., Herrmann, H., Kanakidou, M., Kelly, J. T., Ku, I. T., McNeill, V. F., Riemer, N., Schaefer, T., Shi, G., Tilgner, A., Walker, J. T., Wang, T., Weber, R., Xing, J., Zaveri, R. A., and Zuend, A.: The acidity of atmospheric particles and clouds, *Atmos. Chem. Phys.*, 20, 4809-4888, 10.5194/acp-20-4809-2020, 2020.
- 610 Seinfeld, J. H., and Pandis, S. N.: Atmospheric chemistry and physics: from air pollution to climate change, John Wiley & Sons, Inc., Hoboken, xxviii + 1203 pp. pp., 2006.
- Shen, H. Z., Tao, S., Liu, J. F., Huang, Y., Chen, H., Li, W., Zhang, Y. Y., Chen, Y. C., Su, S., Lin, N., Xu, Y. Y., Li, B. G., Wang, X. L., and Liu, W. X.: Global lung cancer risk from PAH exposure highly depends on emission sources and individual susceptibility, *Scientific Reports*, 4, 10.1038/srep06561, 2014.
- 615 Shi, G., Xu, J., Peng, X., Xiao, Z., Chen, K., Tian, Y., Guan, X., Feng, Y., Yu, H., Nenes, A., and Russell, A. G.: pH of Aerosols in a Polluted Atmosphere: Source Contributions to Highly Acidic Aerosol, *Environ Sci Technol*, 51, 4289-4296, 10.1021/acs.est.6b05736, 2017.
- Shi, X., Nenes, A., Xiao, Z., Song, S., Yu, H., Shi, G., Zhao, Q., Chen, K., Feng, Y., and Russell, A. G.: High-Resolution Data Sets Unravel the Effects of Sources and Meteorological Conditions on Nitrate and Its Gas-Particle Partitioning, *Environ Sci*
- 620 *Technol*, 53, 3048-3057, 10.1021/acs.est.8b06524, 2019.
- Sickles, I. J. E., Hodson, L. L., and Vorburger, L. M.: Evaluation of the filter pack for long-duration sampling of ambient air, *Atmospheric Environment*, 33, 2187-2202, [https://doi.org/10.1016/S1352-2310\(98\)00425-7](https://doi.org/10.1016/S1352-2310(98)00425-7), 1999.
- Sickles, J. E., and Shadwick, D. S.: Comparison of particulate sulfate and nitrate at collocated CASTNET and IMPROVE sites in the eastern US, *Atmospheric Environment*, 42, 2062-2073, <https://doi.org/10.1016/j.atmosenv.2007.11.051>, 2008.
- 625 Song, S., Gao, M., Xu, W., Shao, J., Shi, G., Wang, S., Wang, Y., Sun, Y., and McElroy, M. B.: Fine-particle pH for Beijing winter haze as inferred from different thermodynamic equilibrium models, *Atmos. Chem. Phys.*, 18, 7423-7438, 10.5194/acp-18-7423-2018, 2018.
- Song, S., Nenes, A., Gao, M., Zhang, Y., Liu, P., Shao, J., Ye, D., Xu, W., Lei, L., Sun, Y., Liu, B., Wang, S., and McElroy, M. B.: Thermodynamic Modeling Suggests Declines in Water Uptake and Acidity of Inorganic Aerosols in Beijing Winter Haze
- 630 Events during 2014/2015–2018/2019, *Environmental Science & Technology Letters*, 6, 752-760, 10.1021/acs.estlett.9b00621, 2019.
- Surratt, J. D., Chan, A. W. H., Eddingsaas, N. C., Chan, M., Loza, C. L., Kwan, A. J., Hersey, S. P., Flagan, R. C., Wennberg, P. O., and Seinfeld, J. H.: Reactive intermediates revealed in secondary organic aerosol formation from isoprene, *Proceedings of the National Academy of Sciences*, 107, 6640, 10.1073/pnas.0911114107, 2010.
- 635 Tao, Y., and Murphy, J. G.: The sensitivity of PM<sub>2.5</sub> acidity to meteorological parameters and chemical composition changes: 10-year records from six Canadian monitoring sites, *Atmos. Chem. Phys.*, 19, 9309-9320, 10.5194/acp-19-9309-2019, 2019.
- Theobald, M. R., Simpson, D., and Vieno, M.: Improving the spatial resolution of air-quality modelling at a European scale—development and evaluation of the Air Quality Re-gridder Model (AQR v1. 1), *Geoscientific Model Development*, 9, 4475-4489, 2016.
- 640 United States Environmental Protection Agency: Clean Air Status and Trends Network (CASTNET), in, <https://www.epa.gov/castnet>.
- 2011 National Emissions Inventory (NEI) Data: <https://www.epa.gov/air-emissions-inventories/2011-national-emissions-inventory-nei-data>, 2012a.
- United States Environmental Protection Agency: CASTNET Quality Assurance Quarterly Report, United States Environmental
- 645 Protection Agency, 2012b.

- United States Environmental Protection Agency: CMAQ (Version 5.0.2) [Software], in, 2014.
- Vasilakos, P., Russell, A., Weber, R., and Nenes, A.: Understanding nitrate formation in a world with less sulfate, *Atmos. Chem. Phys.*, 18, 12765-12775, 10.5194/acp-18-12765-2018, 2018.
- 650 Wang, G., Zhang, R., Gomez, M. E., Yang, L., Levy Zamora, M., Hu, M., Lin, Y., Peng, J., Guo, S., Meng, J., Li, J., Cheng, C., Hu, T., Ren, Y., Wang, Y., Gao, J., Cao, J., An, Z., Zhou, W., Li, G., Wang, J., Tian, P., Marrero-Ortiz, W., Secrest, J., Du, Z., Zheng, J., Shang, D., Zeng, L., Shao, M., Wang, W., Huang, Y., Wang, Y., Zhu, Y., Li, Y., Hu, J., Pan, B., Cai, L., Cheng, Y., Ji, Y., Zhang, F., Rosenfeld, D., Liss, P. S., Duce, R. A., Kolb, C. E., and Molina, M. J.: Persistent sulfate formation from London Fog to Chinese haze, *Proceedings of the National Academy of Sciences*, 113, 13630-13635, 10.1073/pnas.1616540113, 2016.
- 655 Wang, R., Tao, S., Balkanski, Y., Ciais, P., Boucher, O., Liu, J., Piao, S., Shen, H., Vuolo, M. R., Valari, M., Chen, H., Chen, Y., Cozic, A., Huang, Y., Li, B., Li, W., Shen, G., Wang, B., and Zhang, Y.: Exposure to ambient black carbon derived from a unique inventory and high-resolution model, *Proceedings of the National Academy of Sciences*, 111, 2459-2463, 10.1073/pnas.1318763111, 2014a.
- 660 Wang, S., Wang, L., Li, Y., Wang, C., Wang, W., Yin, S., and Zhang, R.: Effect of ammonia on fine-particle pH in agricultural regions of China: comparison between urban and rural sites, *Atmos. Chem. Phys.*, 20, 2719-2734, 10.5194/acp-20-2719-2020, 2020.
- Wang, Y., Ying, Q., Hu, J., and Zhang, H.: Spatial and temporal variations of six criteria air pollutants in 31 provincial capital cities in China during 2013–2014, *Environment International*, 73, 413-422, <https://doi.org/10.1016/j.envint.2014.08.016>, 2014b.
- Wang, Y., Gong, Z., Liu, Z. L., Tang, G., Cheng, L., Che, F., Gao, J., and Ji, D.: Construction and Application of Comprehensive Observation Network for Air
- 665 Pollution in Beijing-Tianjin-Hebei and Its Surrounding Areas(In Chinese), *Environmental Science Research*, 32, 1651-1663, 10.13198/j.issn.1001-6929.2019.09.12, 2019.
- Weber, R. J., Guo, H. Y., Russell, A. G., and Nenes, A.: High aerosol acidity despite declining atmospheric sulfate concentrations over the past 15 years, *Nat Geosci*, 9, 282-+, 10.1038/Ngeo2665, 2016.
- William C. Skamarock , J. B. K., Jimy Dudhia , David O. Gill , Dale M. Barker , Wei Wang , Jordan G. Powers: A description of the Advanced Research WRF version 3. NCAR Technical note -475+STR, 2008.
- 670 Xie, Y., Wang, G., Wang, X., Chen, J., Chen, Y., Tang, G., Wang, L., Ge, S., Xue, G., Wang, Y., and Gao, J.: Nitrate-dominated PM<sub>2.5</sub> and elevation of particle pH observed in urban Beijing during the winter of 2017, *Atmos. Chem. Phys.*, 20, 5019-5033, 10.5194/acp-20-5019-2020, 2020.
- 675 Yao, X., Chan, C. K., Fang, M., Cadle, S., Chan, T., Mulawa, P., He, K., and Ye, B.: The water-soluble ionic composition of PM<sub>2.5</sub> in Shanghai and Beijing, China, *Atmospheric Environment*, 36, 4223-4234, [https://doi.org/10.1016/S1352-2310\(02\)00342-4](https://doi.org/10.1016/S1352-2310(02)00342-4), 2002.
- Yarwood, G., Rao, S., Yocke, M. A., and Whitten, G. Z.: Updates to the Carbon Bond Chemical Mechanism: CB05, 2005.
- 680 Ye, D., Klein, M., Mulholland, J. A., Russell, A. G., Weber, R., Edgerton, E. S., Chang, H. H., Sarnat, J. A., Tolbert, P. E., and Ebel Sarnat, S.: Estimating Acute Cardiovascular Effects of Ambient PM(2.5) Metals, *Environ Health Perspect*, 126, 027007, 10.1289/ehp2182, 2018.
- Zhang, Q., Streets, D. G., He, K., and Klimont, Z.: Major components of China's anthropogenic primary particulate emissions, *Environmental Research Letters*, 2, 045027, 10.1088/1748-9326/2/4/045027, 2007.
- Zhang, Q., Zheng, Y., Tong, D., Shao, M., Wang, S., Zhang, Y., Xu, X., Wang, J., He, H., Liu, W., Ding, Y., Lei, Y., Li, J., Wang, Z., Zhang, X., Wang, Y., Cheng, J., Liu, Y., Shi, Q., Yan, L., Geng, G., Hong, C., Li, M., Liu, F., Zheng, B., Cao, J., Ding, A.,

- 685 Gao, J., Fu, Q., Huo, J., Liu, B., Liu, Z., Yang, F., He, K., and Hao, J.: Drivers of improved PM<sub>2.5</sub>; air quality in China from 2013 to 2017, *Proceedings of the National Academy of Sciences*, 116, 24463, 10.1073/pnas.1907956116, 2019.
- Zhang, R., Jing, J., Tao, J., Hsu, S. C., Wang, G., Cao, J., Lee, C. S. L., Zhu, L., Chen, Z., Zhao, Y., and Shen, Z.: Chemical characterization and source apportionment of PM<sub>2.5</sub> in Beijing: seasonal perspective, *Atmos. Chem. Phys.*, 13, 7053-7074, 10.5194/acp-13-7053-2013, 2013.
- 690 Zhang, T., Cao, J., Tie, X., Shen, Z., Liu, S. X., Ding, H., Han, Y., Wang, G., Ho, K. F., Qiang, J., and Li, W. T.: Water-soluble ions in atmospheric aerosols measured in Xi'an, China: Seasonal variations and sources, *Atmospheric Research*, 102, 110-119, 10.1016/j.atmosres.2011.06.014, 2011.
- Zheng, G., Su, H., Wang, S., Andreae, M. O., Pöschl, U., and Cheng, Y.: Multiphase buffer theory explains contrasts in atmospheric aerosol acidity, *Science*, 369, 1374, 10.1126/science.aba3719, 2020.
- 695 Zheng, G. J., Duan, F. K., Su, H., Ma, Y. L., Cheng, Y., Zheng, B., Zhang, Q., Huang, T., Kimoto, T., Chang, D., Pöschl, U., Cheng, Y. F., and He, K. B.: Exploring the severe winter haze in Beijing: the impact of synoptic weather, regional transport and heterogeneous reactions, *Atmos. Chem. Phys.*, 15, 2969-2983, 10.5194/acp-15-2969-2015, 2015.

700

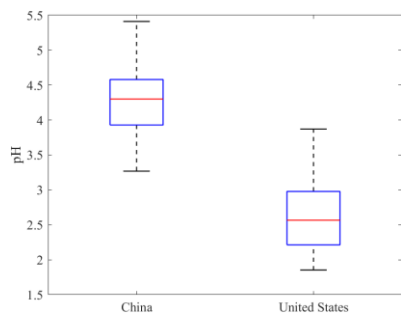


**Figure 1.** Annual average aerosol pH at each monitoring site in China and the United States based on observational data. The arithmetic mean (midline), the interquartile range (box), and the minimum-maximum range (whiskers) are shown in the box plot.

705

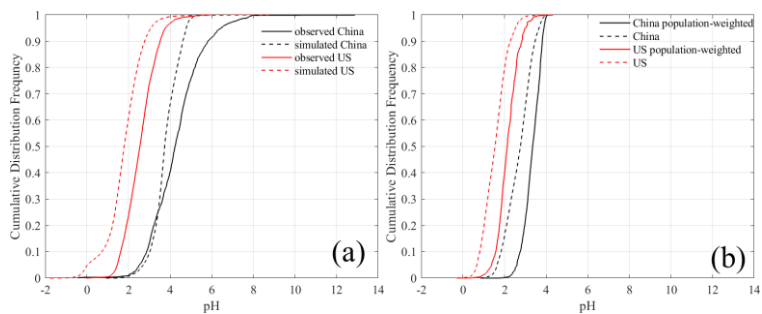


**Figure 2.** The cumulative distribution function (CDF) curves of aerosol pH in China and the United States based on (a) observed particulate and gaseous composition (solid lines) and CMAQ simulations collocated with observation sites (dashed line); (b) simulated data nationwide. In panel (b), both average and population weighted CDFs are shown.

710

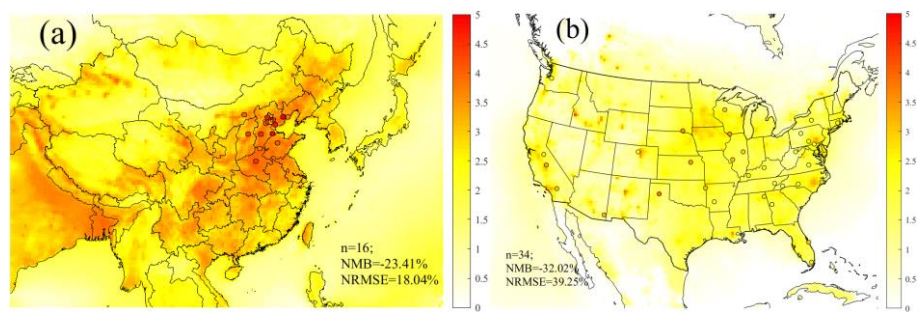


**Figure 3.** Overlay of annual mean pH calculated based on simulated concentrations (colored map) and observed concentrations (colored dots) over the study domain in (a) China and (b) the United States. Number of sites (N), normalized mean bias (NMB) and normalized root-mean-square error (NRMSE) are provided in each figure.

715

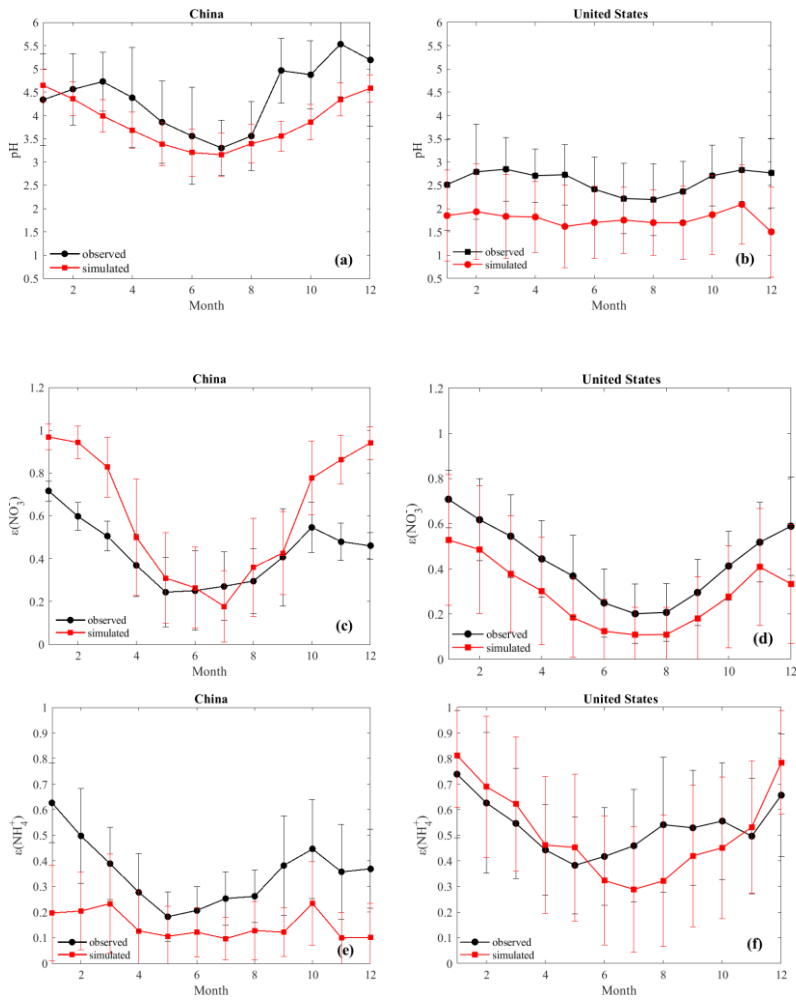
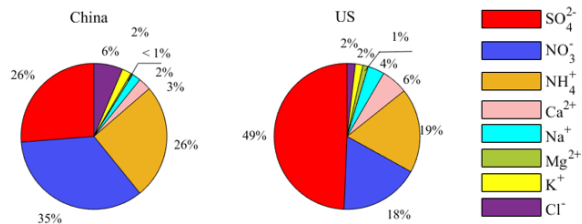
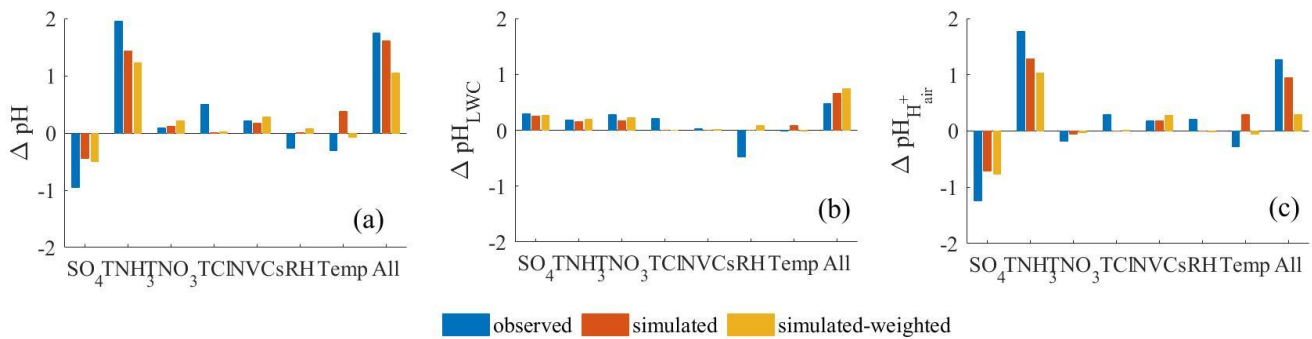


**Figure 4.** Monthly average values of pH,  $\epsilon(\text{NO}_3^-)$  and  $\epsilon(\text{NH}_4^+)$  based on observed and CMAQ simulated data in China (a, c, e) and in the United States (b, d, f). The error bars represent the standard deviation of all the cases in each month.



720 **Figure 5.** Annual average values of water-soluble ions (WSI) concentration profiles in China (left) and in the United States (right).



725 **Figure 6. Contributions of individual components and meteorological factors to (a) total difference of aerosol pH ( $\Delta pH$ ), (b) the aerosol pH difference through the pathway of LWC ( $\Delta pH_{LWC}$ ), and (c) the aerosol pH difference through the pathway of  $H^+$  air ( $\Delta pH_{H^+}$ ) between China and the United States calculated by multi-variable Taylor series method (MTSM) in Sect. 2.4. For each factor, the sum of the contributions through the two pathways yields the net contribution of this factor to the aerosol pH. The case in the United States is chosen as the starting point, and China as the ending point.**

730 **Table 1. Summary of the one-year average values of mass concentration of water-soluble ions (WSI), gaseous and aerosol species, aerosol pH and meteorological parameters (as average  $\pm$  standard deviation) in China and the United States during the study periods (i.e., 2017 for China and 2011 for the United States).**

	China(n=1845)	US(n=1191)
<b>WSI (<math>\mu\text{g m}^{-3}</math>)</b>	34.4 $\pm$ 25.5	5.7 $\pm$ 2.2
<b>Temperature (K)</b>	284.8 $\pm$ 11.7	287.4 $\pm$ 10.0
<b>RH (%)</b>	45.1 $\pm$ 17.6	71.4 $\pm$ 20.9
<b>pH</b>	4.3 $\pm$ 1.2	2.6 $\pm$ 0.7
<b>Particle phase (<math>\mu\text{g m}^{-3}</math>)</b>		
<b>SO<sub>4</sub><sup>2-</sup></b>	9.2 $\pm$ 7.1	2.2 $\pm$ 1.3
<b>NO<sub>3</sub><sup>-</sup></b>	12.1 $\pm$ 11.1	0.8 $\pm$ 0.9
<b>NH<sub>4</sub><sup>+</sup></b>	8.9 $\pm$ 8.0	0.8 $\pm$ 0.5
<b>Cl<sup>-</sup></b>	2.2 $\pm$ 2.3	0.4 $\pm$ 0.1
<b>Na<sup>+</sup></b>	0.7 $\pm$ 1.0	0.2 $\pm$ 0.2
<b>K<sup>+</sup></b>	0.7 $\pm$ 0.6	0.1 $\pm$ 0.1
<b>Ca<sup>2+</sup></b>	1.0 $\pm$ 0.1	0.3 $\pm$ 0.2
<b>Mg<sup>2+</sup></b>	0.2 $\pm$ 0.1	0.1 $\pm$ 0.1
<b>Gaseous phase (<math>\mu\text{g m}^{-3}</math>)</b>		
<b>NH<sub>3</sub></b>	18.0 $\pm$ 12.6	1.1 $\pm$ 1.7
<b>HCl</b>	1.9 $\pm$ 3.4	-
<b>HNO<sub>3</sub></b>	1.0 $\pm$ 1.1	1.0 $\pm$ 0.6
<b>Total (<math>\mu\text{g m}^{-3}</math>)</b>		
<b>TNH<sub>3</sub></b>	26.5 $\pm$ 17.2	1.9 $\pm$ 1.8
<b>TCl</b>	4.1 $\pm$ 4.5	-
<b>TNO<sub>3</sub></b>	13.1 $\pm$ 11.2	1.8 $\pm$ 1.1

735